Bioorganic & Medicinal Chemistry Letters 20 (2010) 1491–1495

Contents lists available at ScienceDirect

Bioorganic & Medicinal Chemistry Letters

journal homepage: www.elsevier.com/locate/bmcl

The discovery and optimization of hexahydro-2*H*-pyrano[3,2-*c*]quinolines (HHPQs) as potent and selective inhibitors of the mitotic kinesin-5

Kai Schiemann [a,*], Dirk Finsinger [b], Frank Zenke [c], Christiane Amendt [d], Thorsten Knöchel [e], David Bruge [b], Hans-Peter Buchstaller [b], Ulrich Emde [b], Wolfgang Stähle [b], Soheila Anzali [f]

[a] MS-RTC-MedChem DA35, Merck Serono, Merck KGaA, Frankfurter Strasse 250, D-64293 Darmstadt, Germany
[b] MS-RTC-MedChem, Merck Serono, Merck KGaA, Frankfurter Strasse 250, D-64293 Darmstadt, Germany
[c] MS-ROB-Cellular Pharmacology, Merck Serono, Merck KGaA, Frankfurter Strasse 250, D-64293 Darmstadt, Germany
[d] MS-ROV-DA-in vivo Pharmacology, Merck Serono, Merck KGaA, Frankfurter Strasse 250, D-64293 Darmstadt, Germany
[e] MS-RES, Merck Serono, Merck KGaA, Frankfurter Strasse 250, D-64293 Darmstadt, Germany
[f] PC-RT Computer Modeling, Merck KGaA, Frankfurter Strasse 250, D-64293 Darmstadt, Germany

ARTICLE INFO

Article history:
Received 17 December 2009
Revised 19 January 2010
Accepted 20 January 2010
Available online 25 January 2010

Keywords:
Kinesin-5
Eg5 inhibitors
Kinesin spindle protein
KSP
Anti mitotic agents
SAR
EMD 534085

ABSTRACT

Here we describe the discovery and optimization of hexahydro-2*H*-pyrano[3,2-*c*]quinolines (HHPQs) as potent and selective inhibitors of the mitotic kinesin-5 originally found during a high-throughput screening (HTS) campaign sampling our in-house compound collection. The compounds optimized subsequently and characterized herein were potently inhibiting the ATPase activity of Kinesin-5 and also exhibited consistent cellular activity, in that cells arrested in mitosis and apoptosis induction could be observed. X-ray crystallographic data demonstrated that these inhibitors bind in an allosteric pocket of Kinesin-5 distant from the nucleotide and microtubule binding sites. The selected clinical candidate **EMD 534085** caused strong growth inhibition in human tumor xenograft models using Colo 205 colon carcinoma cells at doses below 30 mg/kg administered twice weekly without showing severe toxicity as determined by loss of body weight.

The process of mitosis is a highly attractive point of therapeutic intervention in cancer therapy and a variety of antimitotic drugs are successfully being used in the clinic.[1] Especially microtubule targeting inhibitors are highly efficacious; however, these drugs are associated with a variety of side effects,[2] including peripheral neuropathies.[3] Moreover, the clinical efficacy of antimitotic drugs has been hampered due to the development of drug resistance. Therefore, it is of great interest to identify novel antimitotic therapeutics with alternate mechanisms of actions to either eliminate or reduce neurotoxicities as well circumvent drug resistance. Several potential new targets (e.g., mitotic kinases, kinesin ATPases) have been identified and are currently in preclinical and clinical development by many pharmaceutical companies.[4]

The mitotic kinesin-5 (KSP, KIF11, Eg5) belongs to this group of novel antimitotic targets. Kinesins are ATP-dependent motor proteins which transport cargoes along the microtubule or participate in chromosome or spindle movements.[5] Mitotic kinesins function during mitosis only. The mitotic kinesin-5 is essential for proper mitotic spindle formation.[6] Kinesin-5 interacts with the spindle and is thought to stabilize the bipolar architecture of the spindle apparatus.[7] The first identified inhibitor against Kinesin-5 was Monastrol, discovered by the groups of Stuart Schreiber and Tim Mitchison.[8] Analysis of Monastrol's mode of action has shown that the activity to hydrolyze ATP is absolutely required for its proper function.[9] The typical phenotype caused by kinesin-5 inhibition such as M phase arrest with characteristic monoastral spindles in cancer cells was nicely shown applying **EMD 534085** and other kinesin-5 inhibitors.[9c]

Here, we describe the discovery and optimization of hexahydro-2*H*-pyrano[3,2-*c*]quinolines (HHPQs) as potent and selective inhibitors of the mitotic kinesin-5 originally identified in the high-throughput screening (HTS). We were able to further optimize our initially discovered inhibitors to high potency and selectivity in line with consistent cellular mechanism of action. Protein X-ray structures of kinesin-5 in complex with ADP and several HHPQs demonstrate that these inhibitors bind in an allosteric pocket of Kinesin-5 distant from the nucleotide and microtubule binding sites.

Small molecule inhibitors of Kinesin-5 were found in a HTS of our in-house compound collection. An in vitro ATPase assay in the presence of microtubules measuring the compound's ability

* Corresponding author. Tel.: +49 6151728139; fax: +49 6151723129.
E-mail address: kai.schiemann@merck.de (K. Schiemann).

0960-894X/$ - see front matter © 2010 Elsevier Ltd. All rights reserved.
doi:10.1016/j.bmcl.2010.01.110

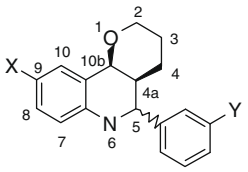

1	X=Y=H	IC50 > 10 μM
2	X=*tert.*-Bu, Y=H	IC50 = 300 nM
3	X=*tert.*-Bu, Y=F	IC50 = 870 nM
4	X=*tert.*-Bu, Y=Cl	IC50 > 10 μM

Figure 1. HHPQs as kinesin-5 inhibitors.

to prevent the hydrolysis of ATP to ADP was established, providing a simple and robust biochemical assay to determine the potency of enzyme inhibition.[10]

In an initial HTS screen around 1000 HHPQs out of 232,000 compounds were tested, of which 40 confirmed hits were identified. A R-group analysis showed clearly that the 9-position of the HHPQs plays an important role for the activity as indicated for compound **2** with a *tert*-butyl group (Fig. 1, IC_{50} = 300 nM) compared to the non-substituted compound **1** (IC_{50} >10 μM). As well, steric restrictions in the phenyl substituent of the molecule were identified; the potency dropped dramatically by exchanging a fluoro by a chloro substituent (compounds **3** and **4**).

The HHPQs were readily assembled by modification of the Povarov reaction[11] as shown in Scheme 1. The inverse electron-demand aza Diels–Alder reaction worked well with a wide range of anilines and aromatic aldehydes with dihydropyran in a one-pot reaction using 1 equiv of TFA at room temperature. The product mixture contained 2 diastereomers mainly in favor of the *trans*-product. Many publications described this reaction by variation of the Brønsted[12] or Lewis[13] acid catalyst and solvent.[14] Others induce the reaction photochemically[15] or describe solid-supported[16] or stereoselective approaches[17] to the compound class. In our case the two diastereomers could be easily separated by chromatography or crystallization. Since we could show that the *trans*-isomer is more stable and potent than the *cis*-isomer (easily forms compound **9**, also isolated in various yields as a side product during the reaction) the SAR is described for the racemic *trans*-isomer. For example, *trans*-isomer **31** (Table 2) expressing a kinesin-5 activity of IC_{50} = 40 nM is five times more potent than its corresponding *cis*-isomer, as well as *trans*-isomer **44**, which is 3 times more potent than its *cis*-isomer.

Looking at the SAR shown in Table 1 one can easily see that a spherical hydrophobic substituent at the C-9 position gives the most potent compounds in accordance to the protein X-ray structure of kinesin-5 in complex with **EMD 534085** (Fig. 2),[18] which can also be compared to co-crystal structures of several other inhibitors described in the literature.[19] The aromatic portion in the western part in addition with a non-lipophilic *tert*-butyl substituent at C-9 (compound **15**, Table 1) fills-up perfectly the hydrophobic pocket of the allosteric binding site of the kinesin-5 protein. The potency dropped when the steric bulkiness was reduced from *tert*-butyl to isopropyl (**14**) to ethyl (**12**) to methyl (**11**) and chlorine (**18**) or—in opposite—was increased (e.g., *n*-Pr, **13**). The CF_3 derivative appeared to be equally potent (**16**). In agreement with structural information obtained by protein X-ray crystallography, all attempts to introduce more polar substituents, like nitriles (**19**, **20**), amines (**23**), alcohols (**24**) or even acid functions (**22**) let to less active or inactive compounds. All efforts to vary the position of the hydrophobic group in the western part or to introduce additional substituents also reduced the potency dramatically. Only fluorine in 7-position was accepted and in-

Table 1
Western part SAR

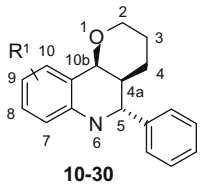

10-30

Entry	R^1	Kinesin-5 IC_{50} (nM)	Proliferation in HCT116 IC_{50} (nM)
10	H	>10,000	n.d.[a]
11	9-Me	420	840
12	9-Et	130	370
13	9-*n*-Pr	360	1800
14	9-*i*-Pr	130	170
15	9-*tert*-Bu	120	250
16	9-CF_3	110	280
17	9-SF_5	910	3400
18	9-Cl	720	1400
19	9-CN	>10,000	n.d.[a]
20	9-CH_2CN	500	580
21	9-OCF_3	3700	>10,000
22	9-COOH	>10,000	n.d.[a]
23	9-NMe_2	5300	8600
24	9-$(CH_2)_2OH$	10,000	>10,000
25	8-*tert*-Bu	>10,000	n.d.[a]
26	7-F,9-CF_3	90	130
27	7-F,8-Cl	540	1600
28	8,9-Di-Me	1250	1500
29	7,9-Di-Me	>10,000	n.d.[a]
30	8,10-Di-Me	>10,000	n.d.[a]

[a] Not determined.

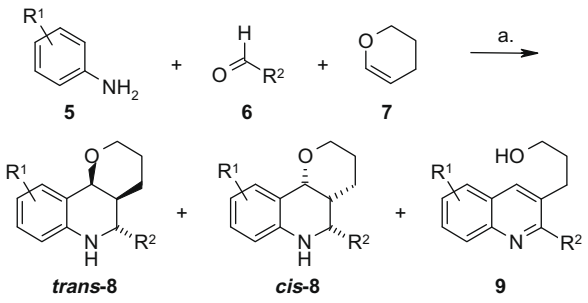

5 **6** **7**

***trans*-8** ***cis*-8** **9**

Scheme 1. Synthesis of basic HHPQs. Reagents and conditions: (a) trifluoroacetic acid (1 equiv), acetonitrile, 0–5 °C→rt, 4 h.

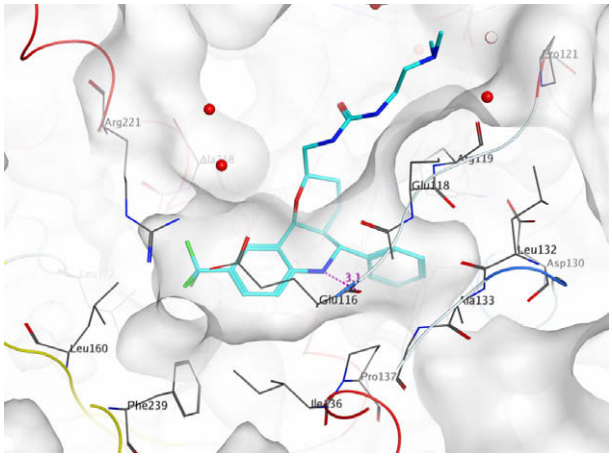

Figure 2. X-ray structure of **EMD 534085** in the allosteric binding pocket of kinesin-5.

Table 2
Eastern part SAR

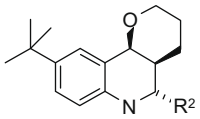

15, 31-50

Entry	R^2	Kinesin-5 IC_{50} (nM)	Proliferation in HCT116 IC_{50} (nM)
15	Ph	120	250
31	3-OH-Ph	40	40
32	4-OH-Ph	34	32
33	3-OH,4-OH-Ph	95	320
34	3-F, 4-OH-Ph	17	19
35	3-F,4-OMe-Ph	>10,000	n.d.[a]
36	4-(NH-COMe)-Ph	>10,000	n.d.[a]
37	3-NH_2-Ph	2300	7000
38	4-COOH-Ph	>10,000	n.d.[a]
39	2-F-Ph	170	260
40	4-F-Ph	270	970
41	3-F-Ph	350	1800
42	3-Cl-Ph	6800	>10,000
43	2-Thiophenyl	25	20
44	3-Thiophenyl	120	130
45	5-Cl-2-Thiophenyl	300	880
46	2-Imidazolyl	>10,000	>10,000
47	2-Thioazolyl	530	1600
48	3-Pyridyl	1100	2000
49	*c*-Hexyl	>10,000	n.d.[a]
50	$(CH_2)_4OH$	>10,000	n.d.[a]

[a] Not determined.

creased the potency of the HHPQ kinase-5 inhibitors slightly as exemplified by combination with the trifluoro methyl group of compound **26**.

In the eastern part of the molecule an aromatic moiety was shown to be crucial for the activity, for example, *c*-hexyl (**49**, Table 2) or aliphatic alcohols (**50**) were inactive. In the protein X-ray structure (Fig. 2) the phenyl ring positions deeply into the pocket. In analogy to Monastrol, in which the phenol moiety forms a hydrogen bond to the carbonyl oxygen of the backbone amide bond of Glu118, the corresponding derivatives in the HHPQ series were synthesized. And indeed, the 3-phenolic derivative **31** was three times more potent than the corresponding unsubstituted phenylic compound. Interestingly the 4-phenol **32** was equally potent and by increasing the acidity of the phenol by introducing fluorine in ortho position (**34**) the activity was increased again by a factor of 2. Since larger substituents let to inactive compounds the steric freedom of inhibitors in this part of the allosteric pocket is quite limited, for example, the methoxy derivative of the highly potent phenol **34** expressed decreased activity at least by three orders of magnitude. The anilinic function like in **37** was still tolerated with some loss of activity but amides or acids were completely inactive. Even fluorine-substituted phenyl let to slightly reduced potency (**39**–**41**).

All heterocyclic derivatives containing basic function were inferior compared to compound **15**. Thiazolyl or furanyl derivatives showed already sub-μM activity, whereas thiophene derivatives especially linked at 2-position (**43**) was one of the most active compounds. Further attempts to increase potency of these heterocycles by substitution failed (e.g., **45**).

Conversely to the increased potency, the necessity to fill the hydrophobic protein pocket of the kinesin-5 protein led to poorly soluble compounds, poor PK properties and metabolic instability. As the tetrahydropyran ring points towards the aqueous environment of the protein, which could be nicely shown by analyzing the X-ray structures of kinesin-5 in complex several HHPQ inhibitors (Fig. 2), a position was identified where modifications of these quite small molecules can be done to overcome the mentioned liabilities without loosing the desired activity. The hydroxyl function of a aza Diels–Alder product using commercially available 3,4-dihydro-2*H*-pyran-2-methanol as dienophile—often used in solid-supported chemistry—was supposed to point directly into the aqueous environment. However, these compounds comprised an additional stereogenic center.

Surprisingly, in the course of the aza Diels–Alder reaction only two of the likely four diastereomers (in theory 8 isomers possible) were formed in the reaction, in most cases in a 1:1 mixture as shown in Scheme 2. So far, theoretical consideration did not offer a convincing explanation for this fact. However, as the solubility of ***cis*-53** is much better than of its diastereomer ***trans*-53**, these two compounds could be easily separated by crystallization. ***trans*-53** was separated by chiral HPLC into the enantiomeres[20] or the two antipodes could be separated on a later stage as diastereomeric salts through crystallization.[21] The alcohol function of the enantiomerically pure compound **54** was then activated by selective mesylation and subsequently substituted with amines. The amines for R^4 = H were further derivatized to the amides, sulfonamides, ureas, and carbamates, as described.

The SAR of these modifications is summarized in Table 3. Due to poor PK properties both the phenolic systems (**65**) and the thiophene derivatives (**69**) were abandoned, although these compounds showed a single-digit activity for kinesin-5 and also a strong activity in the HCT116 proliferation assay.[22] Looking at compounds with R^1 = CF_3 and R^2 = Ph all modifications let to highly potent derivatives (**57–62**) with potencies below 20 nM in the ATPase assay. Equally potent are the cyclopropyl (**70**) and isopropyl (**71**) derivatives. Interestingly, a putative analog within this series to Ispinesib[23] (Cytokinetics) was much less active than the other derivatives (compound **63**). The highest potency obtained in the Kinesin-5 assay and the proliferation assay was found for the 7-F, 9-Br or Cl substituted derivatives (**72–76**), outreached by the sulfonamide **76** with IC_{50} values in the range of 1 nM.

The expansion into the aqueous environment did not only improve the potency of the series members, it also improved the solubility, increased the metabolic stability and offered the chance to improve the pharmacokinetic properties.

In a low dose PK of **EMD 534085** in mice the clearance was found to be 1.8 L/h/kg on average, the volume of distribution was 7.4 L/kg and the half life around 2.5 h. The bioavailability in high dose experiments (>10 mg/kg) was always above 50% in mice.

The antitumor activity of **EMD 534085** was determined in vivo using the subcutaneously growing human xenograft Colo205 colon carcinoma model. Two doses of **EMD 534085** (15 mg/kg and 30 mg/kg) were applied twice weekly by ip injection when tumors reached a mean size of approximately 70 mm^3. **EMD 534085** caused a dose-dependent antitumor effect, which was resulting in a complete growth inhibition for the 30 mg/kg dose group (T/C = 19, p <0.001 Anova test) and in a reduced growth rate for the lower dose group (T/C = 62). Both doses of **EMD 534085** were well tolerated as no body weight loss was observed (Fig. 3).

To evaluate selectivity of our identified inhibitors inhibition of other available kinesin family members were tested using the kinesin ATPase endpoint assay format. The superfamily of kinesin ATPases consists of more than hundred representatives which can be ordered into 14 different families. In the human genome 44 kinesins have been identified. **EMD 534085** did not inhibit any other tested kinesins (BimC, CEN-PE, Chromokinesin, KHC, KIF3C, KIFC3, MKLP-1, and MCAK) at 1 μM or 10 μM concentration. Thus, **EMD 534085** appears to selectively inhibit kinesin-5. However, the list of available and tested kinesins is

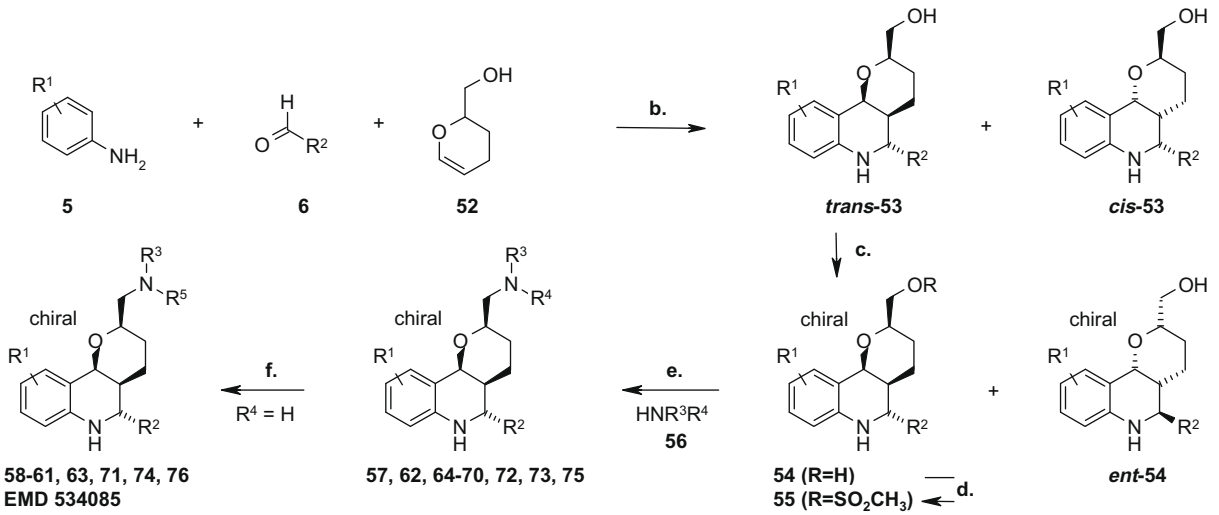

Scheme 2. Synthesis of highly potent enantiomerically pure HHPQs. Reagents and conditions: (b) trifluoroacetic acid (1 equiv), acetonitrile, 0–5 °C→rt, 8 h; (c) HPLC: Chiralpak® AD (ethanol); (d) methane sulfonyl chloride (1 equiv), triethyl amine (2 equiv), methylene chloride, rt, 16 h; (e) HNR^3R^4 (1 equiv), 1-methyl-2-pyrrolidinone, 100 °C, 15 h; (f) various conditions to form amides, sulfonamides, ureas, and carbamates as illustrated in Table 3.

limited and inhibition of other currently inaccessible kinesins cannot be ruled out.

In conclusion, we have described the synthesis and properties of potent and selective kinesin-5 inhibitors in the HHPQ series with high cellular activity. Starting from a high-throughput screen, we were able to rapidly identify Kinesin-5 inhibitors with potencies in the low nanomolar range that possess favorable physical and biological properties. The challenging synthesis due to the high number of stereogenic centers was optimized, although the overall yield is low because of two steps involving diastereomeric and enantioselective separations. The documented SAR could be nicely explained with the X-ray structure of kinesin-5 in complex with **EMD 534085**, which binds to the allosteric pocket of kinesin-5. Intraperitonal administration of **EMD 534085** enabled significant systemic exposure in mice leading to a significant tumor growth reduction without toxic side effects. In combination with a convincing advanced profile and low side effects **EMD 534085** was selected for clinical trials.

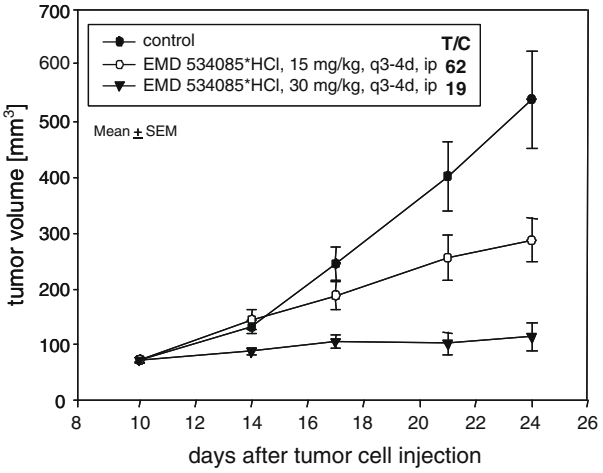

Figure 3. In vivo xenograft model of **EMD 534085** in Colo 205 cells.

Table 3
SAR of the optimized enantiomerically pure HHPQs

Entry	R^1	R^2	R^3	R^4 or R^5	Kinesin-5 IC_{50} (nM)	Proliferation in HCT116 IC_{50} (nM)
57	CF_3	Ph	H	H	20	4
58	CF_3	Ph	H	$C{=}ONH(CH_2)_3OH$	11	11
EMD 534085	CF_3	Ph	H	$C{=}ON(CH)_2NMe_2$	8	30
59	CF_3	Ph	H	$C{=}OO(CH)_2NMe_2$	14	110
60	CF_3	Ph	H	$SO_2(CH_2)_2NHMe$	4	12
61	CF_3	Ph	Me	$SO_2(CH_2)_3NH_2$	7	28
62	CF_3	Ph	Ph	$(CH_2)_2NH_2$	19	25
63	CF_3	Ph	C=O-4-Me-Ph	$(CH_2)_2NH_2$	65	23
64	CF_3	Ph	–N=CH-N=CH-		6	24
65	CF_3	4-OH-Ph	H	Me	4	29
66	CF_3	4-F-Ph	H	Me	58	190
67	*tert*-Bu	Ph	H	Me	4	5
68	*tert*-Bu	Ph	Et	$(CH_2)_2OH$	19	28
69	*tert*-Bu	2-Thiophenyl	H	Me	5	5
70	*c*-Pr	Ph	H	Me	11	8
71	*i*-Pr	Ph	H	$SO_2(CH_2)_3NMe_2$	2	4
72	7-F, 9-Br	Ph	H	Me	3	3
73	7-F, 9-Br	Ph	H	$(CH_2)_2NHC{=}OMe$	6	7
74	7-F, 9-Br	Ph	H	$C{=}O(CH_2)_3NMe_2$	5	16
75	7-F, 9-Cl	Ph	H	$(CH_2)_2OH$	7	19
76	7-F, 9-Cl	Ph	H	$SO_2(CH_2)_2NMe_2$	2	1

Acknowledgment

We thank Dr. Mireille Krier for the illustrations of the inhibitor–protein-interactions.

References and notes

1. (a) Jordan, M. A.; Wilson, L. *Cancer* **2004**, *4*, 253; (b) Pellegrini, F.; Budman, D. R. *Cancer Invest.* **2005**, *23*, 264.
2. Zhou, J.; Giannakakou, P. *Curr. Med. Chem. Anticancer Agents* **2005**, *5*, 65.
3. Bergnes, G.; Brejc, K.; Belmont, L. *Curr. Top. Med. Chem.* **2005**, *5*, 127.
4. (a) Jackson, J. R.; Patrick, D. R.; Dar, M. M.; Huang, P. S. *Nat. Rev. Cancer* **2007**, *7*, 107; (b) Warner, S. L.; Gray, P. J.; Von Hoff, D. D. *Semin. Oncol.* **2006**, *33*, 436; (c) Duhl, D. M.; Renhowe, P. A. *Curr. Opin. Drug Discov. Devel.* **2005**, *8*, 431.
5. Kull, F. J. *Essays Biochem.* **2000**, *35*, 61.
6. (a) Weil, D.; Garcon, L.; Harper, M.; Dumenil, D.; Dautry, F.; Kress, M. *Biotechniques* **2002**, *33*, 1244; (b) Blangy, A.; Lane, H. A.; d'Herin, P.; Harper, M.; Kress, M.; Nigg, E. A. *Cell* **1995**, *83*, 1159.
7. Sawin, K. E.; LeGuellec, K.; Philippe, M.; Mitchison, T. J. *Nature* **1992**, *359*, 540.
8. Mayer, T. U.; Kapoor, T. M.; Haggarty, S. J.; King, R. W.; Schreiber, S. L.; Mitchison, T. J. *Science* **1999**, *286*, 971.
9. (a) Kapoor, T. M.; Mayer, T. U.; Coughlin, M. L.; Mitchison, T. J. *J. Cell. Biol.* **2000**, *150*, 975; (b) Maliga, Z.; Kapoor, T. M.; Mitchison, T. J. *Chem. Biol.* **2002**, *9*, 989; (c) Orth, J. D.; Tang, Y.; Shi, J.; Loy, C. T.; Amendt, C.; Wilm, C.; Zenke, F. T.; Mitchison, T. J. *Mol. Cancer Ther.* **2008**, *7*, 3480.
10. Hydrolysis of ATP was coupled to an ATP regeneration system using an enzyme-coupling to pyruvate kinase and lactate dehydrogenase. As readout the consumption of NADH was measured by a decrease in NADH absorption over time. Tubulin (Cytoskeleton Inc., Denver, Colorado) was polymerized in PEM buffer (80 mM PIPES, 1 mM $MgCl_2$, 1 mM EGTA pH 6.8) by stepwise addition of Paclitaxel and spun through a PEM/40% glycerol cushion to separate the polymerized from non-polymerized tubulin. The Paclitaxel-stabilized microtubules were washed and resuspended in Kinesin-5 reaction buffer (20 mM PIPES, 3 mM $MgCl_2$, 1 mM EGTA, 10 mM NaCl, 20 mM KCl, 0.1% BSA pH 6.8) supplemented with 10 μM Paclitaxel. The Kinesin-5 ATPase reaction was carried out at room temperature in 140 μL Kinesin-5 reaction buffer containing 1 mM DTT, 3 mM ATP, 0.15 mM NADH, 0.48 units pyruvate kinase, 0.47 Units lactate dehydrogenase, 10.5 μg Paclitaxel-stabilized microtubules and 260 ng recombinant Kinesin-5. The total concentration of the Kinesin-5 protein in the reaction was approximately 50 nM. Serial dilutions of compounds were added to the reaction to determine the inhibitory concentration at which 50% of the enzymatic activity was inhibited (IC_{50}). DMSO was used as a solvent for compounds and kept constant in the assay at a concentration of 0.5%. A reaction without the Kinesin-5 ATPase served as a blank control. The ATPase reaction was monitored by measuring absorption at 340 nm over time (Mithras, LB 940 photometer). The reaction velocity was calculated by linear regression from the time kinetic record.
11. Povarov, L. S.; Grigos, V. I.; Karakhanov, R. A.; Mikhailov, B. M. *Br. Acad. Sci. USSR Ch+* **1964**, 163 (*Izv. An. SSSR Khi+* **1964**, 179).
12. (a) Baudelle, R.; Melnyk, P.; Déprez, B.; Tartar, A. *Tetrahedron* **1998**, *54*, 4125; (b) Yadav, J. S.; Subba Reddy, B. V.; Srinivas, R.; Madhuri, C.; Ramalingam, T. *Synlett* **2001**, *2*, 240; (c) Nagarajan, R.; Magesh, C. J.; Perumal, P. T. *Synthesis* **2004**, *1*, 69.
13. (a) Mahesh, M.; Ventakeshwar Reddy, C.; Srinivasa Reddy, K.; Raju, P. V. K.; Narayana Reddy, V. V. *Synth. Commun.* **2004**, *34*, 4089; (b) Ma, Y.; Qian, C.-T.; Xie, M.-H.; Sun, J. *J. Org. Chem.* **1999**, *64*, 6462; (c) More, S. V.; Sastry, M. N. V.; Yao, C.-F. *Synlett* **2006**, *9*, 1399.
14. (a) Vidiš, A.; Ohlin, C. A.; Laurenczy, G.; Küsters, E.; Sedelmeier, G.; Dyson, P. J. *Adv. Synth. Catal.* **2005**, *347*, 266; (b) Jurčik, V.; Wilhelm, R. *Org. Biomol. Chem.* **2005**, *3*, 1239.
15. Zhang, W.; Guo, Y.; Liu, Z.; Jin, X.; Yang, L.; Liu, Z.-L. *Tetrahedron* **2005**, *61*, 1325.
16. Kiselyov, A. S.; Smith, L., II; Virgilio, A.; Armstrong, R. W. *Tetrahedron* **1998**, 7987.
17. (a) Akiyama, T.; Morita, H.; Fuchibe, K. *J. Am. Chem. Soc.* **2006**, *128*, 13070; (b) Magesh, C. J.; Makesh, S. V.; Perumal, P. T. *Bioorg. Med. Chem. Lett.* **2004**, *14*, 2035; (c) Sundarajan, G.; Prabagaran, N.; Varghese, B. *Org. Lett.* **2001**, *3*, 1973.
18. Crystals of Kinesin-5 (amino acids 1–368) in complex with Monastrol were first obtained by vapor diffusion by mixing equal volumes of reservoir solution (17–18% w/v PEG3350, 0.23–0.26 M ammonium citrate pH 7.0) and protein solution (10 mg/ml Kinesin 5, 50 mM PIPES, 2 mM MgCl2, 1 mM EGTA, 1 mM ATP, 1 mM TCEP, 8 mM Monastrol, pH 6.8). Crystals of Kinesin-5 (amino acids 1–368) in complex with **EMD 534085** were subsequently obtained by soaking crystals of Kinesin-5 in complex with Monastrol for 3 days in reservoir solution containing 20 mM **EMD 534085**. X-ray diffraction data were collected at 100 K at beamline X06SA of the Swiss Light Source (Paul-Scherrer-Institut, 5232 Villigen, Switzerland) to 2.0 Å resolution (R-sym = 0.061, completeness = 88,3%) in space group *C*2 with cell dimensions $a = 161.0$ Å, $b = 79.7$ Å, $c = 65.5$ Å, $\alpha = 90°$, $\beta = 96.9°$, $\gamma = 90°$. The structure of Kinesin-5 in complex with **EMD 534085** was determined by difference Fourier analysis and refined to an R-factor of 0.234 and R-free (5% of data) of 0.258. The refined model consists of two copies of Kinesin-5 (visible residues 16–271 and 288–362), ADP (as a result of ATP hydrolysis under the experimental conditions) and **EMD 534085**, related by a twofold non-crystallographic symmetry axis plus water molecules. The coordinates have been deposited with RCSB Protein Data Bank under the accession code 3L9H.
19. (a) Cox, C. D.; Breslin, M. J.; Mariano, B. J.; Coleman, P. J.; Buser, C. A.; Walsh, E. S.; Hamilton, K.; Huber, H. E.; Kohl, N. E.; Torrent, M.; Yan, Y.; Kuo, L. C.; Hartman, G. D. *Bioorg. Med. Chem. Lett.* **2005**, *15*, 2041; (b) Kim, K. S.; Lu, S.; Cornelius, L. A.; Lombardo, L. J.; Borzilleri, R. M.; Schroeder, G. M.; Sheng, C.; Rovnyak, G.; Crews, D.; Schmidt, R. J.; Williams, D. K.; Bhide, R. S.; Traeger, S. C.; McDonnell, P. A.; Mueller, L.; Sheriff, S.; Newitt, J. A.; Pudzianowski, A. T.; Yang, Z.; Wild, R.; Lee, F. Y.; Batorsky, R.; Ryder, J. S.; Ortega-Nanos, M.; Shen, H.; Gottardis, M.; Roussell, D. L. *Bioorg. Med. Chem. Lett.* **2006**, *16*, 3937; (c) Yan, Y.; Sardana, V.; Xu, B.; Homnick, C.; Halczenko, W.; Buser, C. A.; Schaber, M.; Hartman, G. D.; Huber, H. E.; Kuo, L. C. *J. Mol. Biol.* **2004**, *335*, 547.
20. For example, putative separation of 1.3 g of ***trans*-53** with R^1 = Et and R^2 = Ph was carried out on two successive connected 250 × 5 cm IM Chiralpak AD columns with MeOH as mobile phase (flow: 80 mL/min, $\lambda = 254$ nm). The first isomer to elute ($t_R = 8.0$ min, 634 mg), the (−) antipode ($[\alpha]_D^{20}$ −27.1, (*c* 0.94, MeOH)), was active ($IC_{50} = 100$ nM) in the ATPase assay. The second isomer to elute ($t_R = 13.8$ min, 615 mg), the (+) antipode ($[\alpha]_D^{20}$ +27.4, (*c* 0.94, MeOH)), was inactive (IC_{50} >10 μM). Each isomer was >99% ee by analytical HPLC under the same conditions. ^{1}H NMR (500 MHz, DMSO) $\delta = 7.47–7.34$ (m, 4H), 7.34–7.27 (m, 1H), 6.88 (s, 1H), 6.83 (dd, $J = 8.2, 1.9$, 1H), 6.51 (d, $J = 8.2$, 1H), 5.86 (s, 1H), 4.56 (t, $J = 5.8$, 1H), 4.48 (d, $J = 11.4$, 1H), 4.31 (d, $J = 2.2$, 1H), 3.62–3.53 (m, 1H), 3.47–3.41 (m, 1H), 3.39–3.33 (m, 1H), 2.44 (q, $J = 7.6$, 2H), 1.88–1.78 (m, 1H), 1.64–1.55 (m, 1H), 1.53–1.37 (m, 1H), 1.34–1.23 (m, 2H), 1.12 (t, $J = 7.6$, 3H).
21. Schiemann, K.; Emde, U.; Schlueter, T.; Saal, C.; Maiwald, M. PCT WO2007147480A2, 2007.
22. HCT116 cells (ATCC CCL-247) were cultured in MEM alpha medium with 1 mM sodium pyruvate, 2 mM glutamine, and 10% fetal bovine serum. 10,000 cells were plated in a volume of 100 μL in 96-well plates and incubated o/n at 37 °C at 10% CO_2. On the next day, the medium was removed and 100 μL of fresh medium including serial dilutions of compounds were added to the culture plates and incubation was continued further for 48 h. The concentration of the compound solvent DMSO was kept constant at 0.5%. At the end of the compound incubation period the medium was removed and wells were washed briefly with 200 μL 1× PBS. 100 μL crystal violet staining solution (0.5% crystal violet in methanol) was added per well and incubated for 15 min at room temperature. The staining solution was removed and wells were washed thoroughly with deionized water. Plates were dried at room temperature o/n or at 37 °C for 1 h. The remaining dye in the wells was extracted with 200 μL methanol and absorption was determined at 540 or 550 nm.
23. Sorbera, L. A.; Bolos, J.; Serradell, N.; Bayes, M. *Drugs Future* **2006**, *31*, 778.